Support Timing and Ground Stability Analysis for Mine Excavation Using Numerical Modelling

Cui Lin
Process Engineering, Memorial University of Newfoundland, St. John's, Newfoundland & Labrador, Canada
Xinyi Shen
Alamos Gold Inc. Matachewan, Ontario, Canada
D.H. Steve Zou
Civil and Resource Engineering, Dalhousie University, Halifax, NS, Canada

ABSTRACT
The process of underground excavation disrupts field stresses, leading to subsequent stress redistribution and deformation in the rock mass surrounding the excavation. It is of paramount importance to maintain the ground stability in mine operations to ensure safety and sustaining production. To reinforce the rock mass and minimize the potential of ground failure, different rock supports have been utilized to control the deformation and enhance the ground capacity. This paper used numerical modelling in combination with the ground reaction curve and longitudinal deformation profile to determine proper support timing/distance behind an excavation face and assess the effectiveness of installed rock support system. Internal stress reduction was applied as partial replacement of excavation to evaluate the ground response to stress changes. Longitudinal deformation profile along the excavation axis was simulated using an axisymmetric model. In a case study, modelling for the unsupported condition allowed estimate of proper installation distance and required supporting pressure. In the supported conditions, the effectiveness of support was assessed based on the strength factor, deformation and the range of unstable zone. The selected final support pattern ensured elimination of unstable zone around the excavation.

1 INTRODUCTION

Excavation activities in underground mines disturb the natural stress equilibrium in the rock mass. During and after excavation of an opening, significant changes occur in the surrounding rock mass. Initially, the removal of rocks leads to the release of stored stresses within the rock mass (Hoek and Brown 1990, Brady and Brown 2004, Zou 2020). The remaining rock mass has to bear the load that was previously supported by the excavated rock. The excavation process induces stress redistribution within the rock mass, resulting in the development of a zone of increased stress concentration around the opening. This increased stress can cause deformation and fracturing in the immediate vicinity of the excavation, resulting in a damaged zone or "zone of influence". The stress redistribution is not uniform in this zone but varies as the rock mass, adjusting to the new stress regime, depending on many factors such as rock strength, geological structure, and excavation method. The immediate surrounding rock mass may undergo a process of relaxation and exhibit varying degrees of deformation, including convergence towards the opening, dilation, or even collapse.

Accordingly, excavation of an opening in a rock mass induces complex changes in the surrounding rock, including stress redistribution, deformation, and potential damage. Failure to effectively manage deformation can pose significant challenges to ground stability, consequently bringing risks to both the safety of workers and infrastructure.

To control deformation and mitigate these risks, proper design and support measures need to be implemented (Hoek 2001, Martin et al. 2003, Zou 2004, Carranza-Torres and Fairhurst 2009, Kang et al. 2014, Li 2017). The commonly used support system includes rock bolts, shotcrete, steel arches, and mesh, aiming at reinforcing and stabilizing the disturbed rock mass. Deformation and stress analysis is essential for underground excavations and ground support design (Lin and Zou 2021, Lin and Zou 2024). When designing effective support systems, it is necessary to account for the load-deformation behaviors of both the rock mass and the supporting structures (Singh 1992). These elements interact dynamically, striving to achieve equilibrium. To achieve this balance, the support system must exert adequate pressure within a proper timeframe to match the demands imposed by the surrounding rock mass. Therefore, it is crucial to have sufficient understanding of the interaction between rock mass and support system for selecting an appropriate support method and installing support at a proper time. This proactive approach not only enhances the stability of underground mine workings, but also increases mine safety and minimizes the risk of accidents and production disruptions, thereby fostering the long-term sustainability of mining operations.

2 METHODOLOGIES

To determine when the proper time is to install ground support after excavation, the rock mass behavior during stress reduction and the deformation behind the excavation face must be understood. The adopted method integrates the ground reaction curve and the support characteristic curve with the longitudinal deformation profile. With this method, a 2D approach is used to tackle the complex 3D problems (Carranza-Torres and Fairhurst 2000). It offers reasonable approximation and an effective method to estimate the behavior of the rock mass around an excavation and assess the performance of support systems. Additionally, this approach facilitates the strategic planning of timing of support installation. It should be noted that this method is employed under the assumption of a homogeneous and isotropic rock mass, as well as uniform support pressure across the surface of the opening.

2.1 Rock Mass Response to Stress Reduction

Assume that the far-field stress at a distance well ahead of the excavation face is P_o and there is a controllable internal pressure P_i on the surface of the excavated opening. Based on stress reduction, the process of excavation is achieved by reducing the P_o to 0, gradually rather than suddenly, by means of the internal pressure P_i. The deformation of the rock mass during the whole process can thus be simulated by numerical modelling at various internal pressure levels: P_i/P_o = 100%, 90%, … 0% and recorded at the locations of interest in each step. Figure 1 illustrates the radial deformation trajectory on the roof of an opening as the internal stress reduces from P_o to 0. The maximum deformation is reached after P_i has become 0 but before failure.

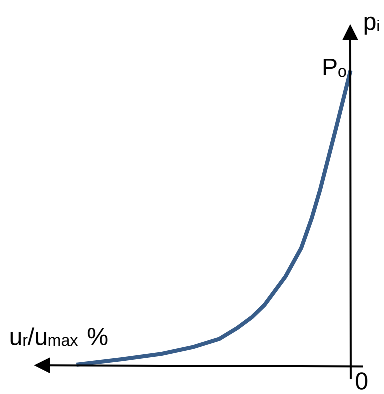

Figure 1. Ground response curve showing the decreasing internal pressure (P_i) and the radial displacement (u_r)

2.2 Longitudinal Deformation Profile

Longitudinal Deformation Profile (LDP) is the radial displacement (u_r) on the excavation boundary as a function of the distance (d) to excavation face (d < 0 ahead of the face and d > 0 behind the face). During excavation of a drift, the initial radial displacement is zero (u_r = 0) at a location far ahead of the excavation face. For a specific location near but behind the excavation face, the excavation face itself bears a portion of the load from the surrounding rock mass, acting as natural support (the face effect). The remaining load is carried by the drift wall behind the excavation face. As advancement continues, the face effect gradually diminishes, transferring the entire load to the drift wall at some distance behind the excavation face. At the same time, the radial displacement increases gradually, eventually reaching the maximum deformation ($u_r = u_{max}$).

The internal pressure P_i resembles the face effect. At the excavation face, P_i is large and at a distance well behind the excavation face, P_i is reduced to 0. The curve in Figure 1 thus resembles the deformation on the roof along the excavation axis. Similar curves can be simulated at any other location as well. The stress and deformation in Figure 1 need to be related to the actual location along the drift.

The longitudinal deformation profile along the excavation axis can be simulated with a pseudo unsupported circular opening. The deformation along a longitudinal line, such as the roof line, is then recorded. The results given in u_r/u_{max} (in %) along the excavation axis are plotted in the upper curve in Figure 2.

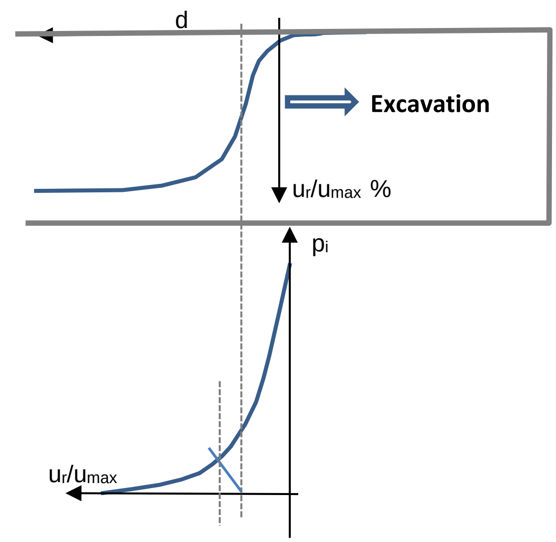

Figure 2. Illustration of support distance from the face at a specified deformation

2.3 Support Strength and Installation Timing

The u_r-P_i curve in Figure 1 can be related to the LDP to determine the proper timing for support installation and the required support strength. This however requires a decision of an acceptable deformation level before installing support. For example, if the deformation of 60% u_{max} is accepted, the remaining deformation must be avoided and a point of u_r/u_{max} = 60% is found on the u_r-P_i curve. The required supporting pressure P_i can be determined at that point. This will be the equilibrium point of supporting, as shown on the lower curve of Figure 2.

A type of support is then selected to match the required supporting pressure. To determine the location of support installation, the stiffness of the selected support is required. The actual value of u_r/u_{max} at installation will be smaller than the specified 60% and can be determined based on the stiffness of the support. On the LDP curve (Figure 2), the point corresponding to the installation point indicates the installation distance from the excavation face for the specified acceptable deformation.

In the following, a case study is presented to demonstrate the above process and to assess the effectiveness of supports.

3 CASE STUDY WITH NUMERICAL SIMULATION

3.1 Model Construction and Calibration

This case is a coal mine drift excavated at a depth of 1300 meters underground, with an excavation opening measuring 3.5 m heigh and 3.8 m wide (Yu et al 2012). The geological formation comprises Fine Sandstone, Coal, and soft Sandy Shale strata. The magnitude of the in-situ stress field around the drift are: major principal stress (σ_H) 46.5 MPa, intermediate principal stress (σ_V) 34.4 MPa, minor principal stress (σ_h) 24.2 MPa. The drift was excavated approximately horizontally along the maximum horizontal stress direction.

Models were developed using a 2-dimensional (2D) finite element program RS2 (Rocscience) to perform simulations. The constitutive relationship for the rock mass material encompasses both elastic and elastoplastic models (Hedayat and Weems 2019). The stresses acting on the cross section of the drift were applied to the model. The failure assessment is based on the Mohr-Coulomb criterion.

To ensure the numerical models closely resemble the real conditions, model calibration was performed. The strength reduction method (Rafiei Renani et al. 2016) and field measurement data were applied to calibrate the model. The unit weight and internal friction angle for the rock were held constant. The iterative process involved decreasing strength parameters by 10% and increasing Poisson's ratio by 5% in each calibration round. If model deformations exceeded the field data, the rock mass properties were set as a lower limit, and properties were increased in the next iteration. Conversely, if model deformations were smaller, the current value became the upper limit, and subsequent estimations were adjusted accordingly. This process continued until displacements in the simulation closely matched the observed field data within an acceptable error.

3.2 Simulation of Ground Response and LDP

To construct the ground reaction curve via the internal pressure reduction method, the internal pressure P_i was segmented into 20 stages. This segmentation involved progressively reducing the internal pressure factor, starting from $P_i/P_o = 1.0$ to eventually $P_i/P_o = 0$. Figure 3 shows the models in two typical stages, depicting the internal pressure within the excavation boundary, acting opposite to the direction of the in-situ stress. The displacement at points of interest was recorded in each step of simulation. The results of displacement of all stages were used to generate the ground response curve (GRC), u_r-P_i, (Figure 5b).

To determine the longitudinal deformation profile, a two-dimensional axisymmetric model of a resembling circular opening was constructed to simplify the problem. Image in a 3D system with XY within the cross section of the drift as shown in Figure 3, Z would be parallel to the drift through the central line where X=Y=0. When the model geometry was rotated around the X axis by 90° within the YZ plane at X = 0, a 2D axisymmetric model would be created, as shown in Figure 4.

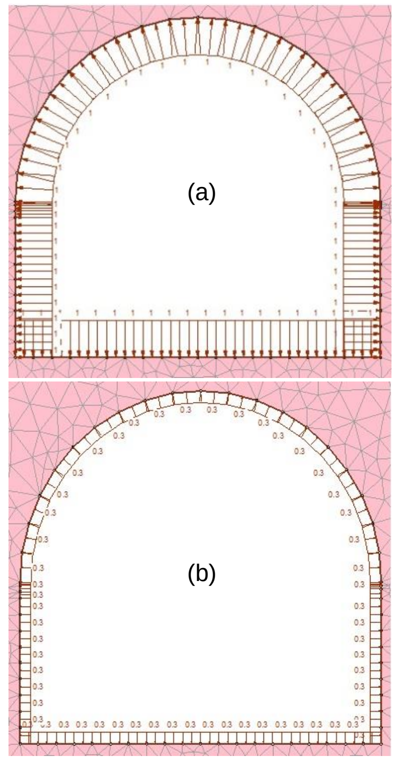

Figure 3. Models with internal pressure inside the excavation boundary opposite to the in-situ stress direction at: (a) P_i/P_o=1 and (b) P_i/P_o = 0.3.

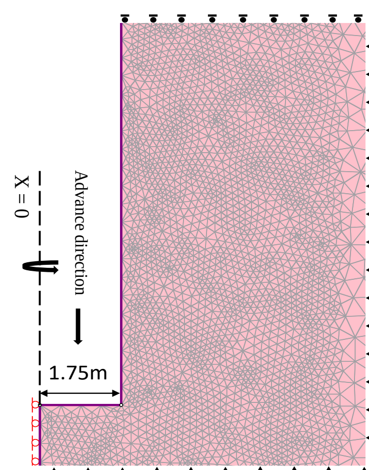

Figure 4. Axisymmetric model of the drift

This model enables approximate simulation of a 3D problem. Displacement query points were selected along the excavation boundary (the roof line in this case) from far behind the face to ahead the face inside the rock mass. The displacement data were then plotted against the drift axis to generate the longitudinal deformation profile (Figure 5a). The normalized displacement (u_r/u_{max}) at a particular location along the drift can be determined based on the d/R value. At the excavation face, d/R = 0, where R is the radius of the resembling drift, and u_r/u_{max} = 0.2.

It is noted that the excavation shape is circular instead of horseshoe shape in the rotated axisymmetric model. However, investigation of the impact of applying a near-circular shape to replace a horseshoe shape in an axisymmetric model by Vlachopoulos and Diederichs (2014) indicated only a minor effect (see Figure 5a), which is not expected to change the overall assessment.

3.3 Assessing Supporting Requirements

At the excavation face, the estimated displacement is 20% u_{max} (Figure 5a). However, it is unlikely to install any support right after excavation at the face. There is some delay, and the deformation would be larger when support is installed. Onsite experience can help determine how much more deformation can be tolerated before support installation.

The displacement at the excavation face can be mapped onto the ground response curve to identify the corresponding stage of stress reduction. In Figure 5b, it is shown P_i/P_o = 0.32. This can be used to assess the requirement of support strength. In this example, P_o is the in-situ vertical stress of 24.2 MPa. The required supporting pressure would be P_i = 0.32 x 24.2 = 7.74 MPa. Apparently, no support can provide that high pressure.

As mentioned above, support, if required, would normally be delayed. A proper type of support is to be selected to match the requirement. Assume that a type of support has been selected, which can provide 1.2 MPa supporting strength. That is the equivalent internal pressure during stress reduction. Then P_i/P_o = 0.05 and the corresponding deformation would be 60% u_{max} (the dotted lines In Figure 5b). This deformation would translate to a distance of d/R = 0.8 in Figure 5a (the dotted lines). That means, d = 0.8 x 3.8m/2 = 1.52 m, the delayed support installation distance behind the excavation face.

The above results would only provide a guideline in assessing support and installation requirements. The exact support and installation timing will require an experienced engineer to make a professional judgement. The supporting capacity of a type of support and the supporting strength of the widely used rock bolts, shotcrete, etc. will vary with many factors and how they are installed. That will be separate topics, not to be discussed here.

4 Assessing Effectiveness of Ground Support

The strength factor (SF), deformation, and depth of plastic/failure zone around the excavated drift can be evaluated with the created numerical models to help assess the effectiveness of installed support system.

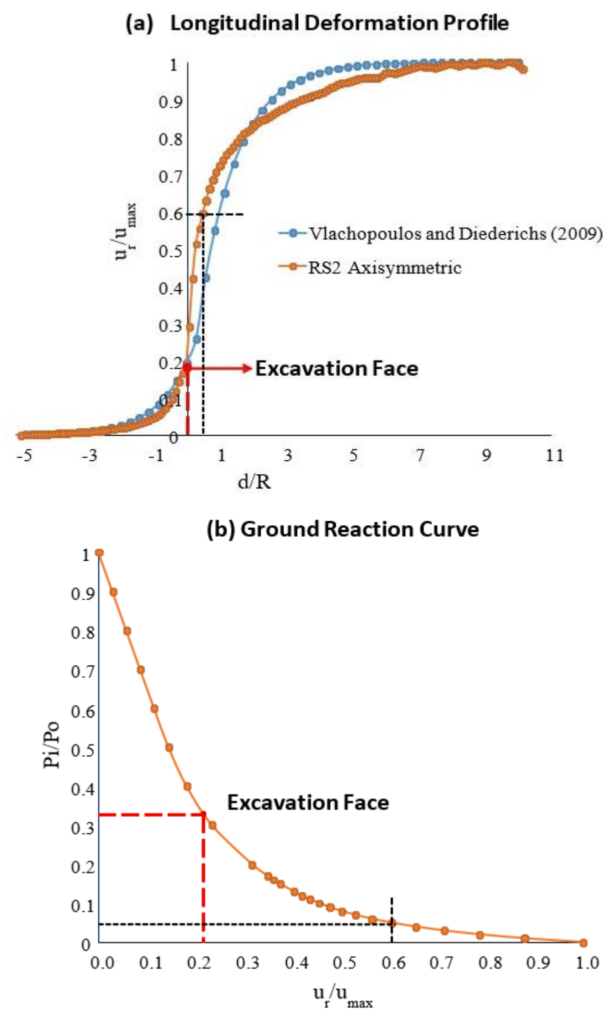

Figure 5. (a) Longitudinal deformation profile, (b) ground response curve: pressure-deformation

Generally, if the SF falls below 1, it indicates instability in elastic analysis. In plastic analysis, it means that the rock mass has been loaded beyond its elastic limit. The depth of the plastic zone, also known as the yielding zone, can also serve as a stability indicator for rock mass around the excavation. Thus, conducting a more precise analysis enables understanding the interaction between support and rock mass.

4.1 Unsupported Drift

First, the unsupported condition was simulated as a base for comparison. The results are depicted in Figure 6. The results from the elastic models (Figure 6a) reveal that the strength factors around the drift after excavation of the new opening are less than 1 (e.g., SF = 0.53 on the floor, SF = 0.62 on the sidewall, and SF = 0.65 on the roof). Notably, the drift floor exhibits the lowest strength factor, indicating the possibility of floor heaving. Several potential factors may contribute to the occurrence of floor heave conditions, including: (1) high vertical-horizontal in-situ stress ratio; (2)

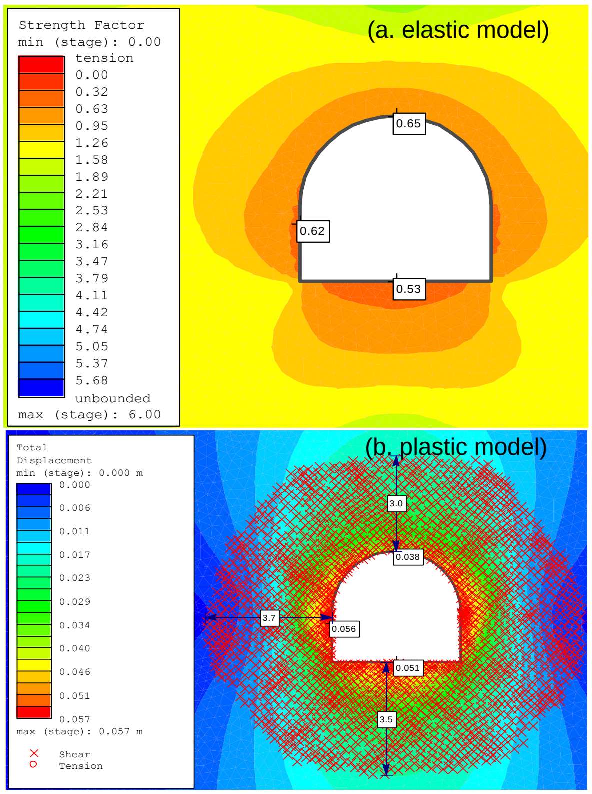

Figure 6. Simulated results for unsupported condition: (a) strength factor, (b) depth of failure zone and displacements around the opening

presence of a weak coal seam layer beneath the drift, necessitating floor support considerations. Overall, strength factor less than 1 indicates unstable conditions for drift opening, and the rock mass would fail.

The results from the plastic model showed an extened yielding zone, which occurred all around drift (Figure 6b). The depth of plastic zone in the rock mass is up to 3.0 meters on the roof, around 3.7 meters into sidewalls, and 3.5 meters in the floor. It can be seen that the vertical displacement on the floor and roof are 5.1 cm and 3.8 cm, respectively. The total vertical displacement (combined roof and floor) for the unsupported case is 8.9 cm, equivalent to 2.54% of the drift height.

Three ground reaction curves for the non-supported condition were generated based on the displacement and stress query points taken at the central location on the floor, the sidewalls, and the roof. The results shown in Figure 7 has captured the fastest-developing displacements on the drift's floor as it has the smallest slope compared to sidewalls and roof. This indicates that the floor is weak, and support is necessary. These curves can aid in analyzing the support installation location and timing separately.

4.2 Rock Bolt Supported Drift

Rock bolting is the typically practiced support system in underground mining operations. In this simulation, pre-tensioned mechanically anchored rock bolts of various lengths and different spacing were tried. With bolts at 8 feet long at 2 feet spacing, failure zone was basically eliminated, and the results are shown in Figure 8.

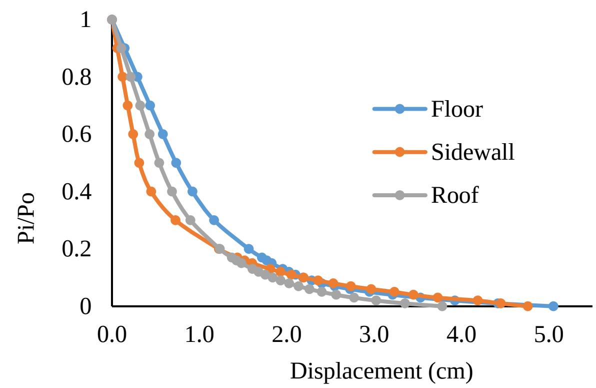

Figure 7. Ground reaction curves for unsupported drift

By taking all three parameters (SF, deformation and depth of failure zone) into account, the rock bolt that has a length of 8 feet with 2 feet spacing gave the satisfactory results in terms of stability, which has the highest strength factor (i.e., FS =1.13) and shallower yielding zone (i.e., 6.36 feet), comparing with other supporting conditions.

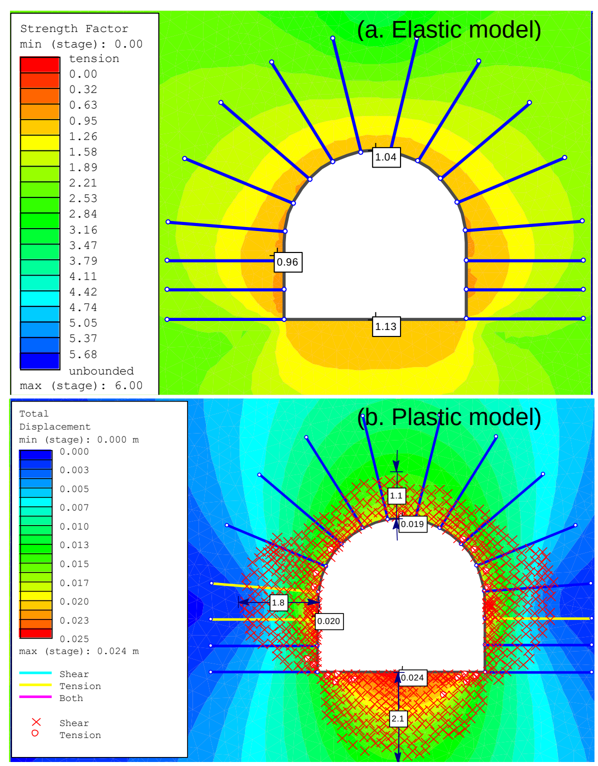

Figure 8. Simulated results for pre-tensioned mechanical bolts with 8 feet length and 2 feet spacing: (a) strength factor, (b) depth of failure zone and displacements around the opening.

In comparison with the unsupported case (Figure 6), unstable zone (SF <0) is almost eliminated, and the depth of yielding zone is significantly reduced. This bolting support seems to be adequate for the drift condition.

As noticed before, floor heaving seems to be a problem and floor bolting was also tried with the same bolting type and pattern. The results Indicated that the strength factor, deformation and depth of yielding zone all slightly improved. Accordingly, support to the drift floor is expected to contribute to stabilizing the entire excavated opening. However, whether the floor is to be supported will be a decision after considering other factors including the cost.

5 Conclusions

This paper aims at exploring ground support requirement and installation timing/distance behind the excavation face. Basic concept and procedure were first introduced, followed by a case study.

Numerical modelling in combination with longitudinal deformation profile provided insights on predicting deformation behind and ahead of the excavation face. The ground reaction curve and the support characteristic curve are utilized to define the critical timing of installing ground support.

To calibrate the numerical model, rock properties were modified by conducting modeling repeatedly until the simulated deformation at the specified locations matched those recorded in the field. Once model was calibrated, deformation at various internal stresses was determined to establish the relationship between support load and deformation. Longitudinal deformation along the excavation axis helped determine the supporting distance from the face at a specified level of acceptable deformation.

To assess the effectiveness of support, simulation was conducted for the unsupported and supported cases. The results were compared based on the strength factor, the depth of failure zone around drift, and the total displacement. Eventually, a suitable support and installation distance were selected.

References

Brady, B.H.G. and Brown, E.T. 2004. Rock Mechanics for Underground Mining, Springer, Dordrecht, Netherlands.

Carranza-Torres, C. and Fairhurst, C. 2000. Application of the Convergence-Confinement Method of Tunnel Design to Rock Masses that Satisfy the Hoek-Brown Failure Criterion. Tunnelling and Underground Space Technology, 15(2): 187-213.

Carranza-Torres, C. and Diederichs, M. 2009. Mechanical Analysis of Circular Liners with Particular Reference to Composite Supports. For example, Liners Consisting of Shotcrete and Steel Sets, Tunnelling and Underground Space Technology, 24(5): 506-532.

Hedayat, A. and Weems, J. 2019. The Elasto-Plastic Response of Deep Tunnels with Damaged Zone and Gravity Effects. Rock Mechanics and Rock Engineering, 52: 5123-5135.

Hoek, E. and Brown, E.T. 1990. Underground Excavations in Rock. CRC Press, Boca Raton, USA.

Hoek, E. 2001. Big Tunnels in Bad Rock. Journal of Geotechnical and Geoenvironmental Engineering, 127(9): 726-740.

Kang, Y.S., Liu, Q.S., Gong, G.Q. and Wang, H.C. 2014. Application of a Combined Support System to the Weak Floor Reinforcement in Deep Underground Coal Mine. International Journal of Rock Mechanics and Mining Sciences, 71: 143-150.

Li, C. 2017. Principles of Rock Bolting Design. Journal of Rock Mechanics and Geotechnical Engineering, 9(3): 396-414.

Lin, C. and Zou, D.H. 2021. Formulation and Verification of 3D In-Situ Stress Estimation Based on Differential-Direction Drilling, *International Journal of Rock Mechanics and Mining Science*, 145: 104833.

Lin, C. and Zou, D.H. 2024. Formulation and Procedure for In Situ Stress Back-analysis from Borehole Strain Changes Measured During Nearby Underground Excavation. *Journal of Rock Mechanics and Geotechnical Engineering*, 15(4): 1031-1943.

Martin, C.D., Kaiser, P.K. and Christiansson, R. 2003. Stress, Instability and Design of Underground Excavations. International Journal of Rock Mechanics and Mining Science, 40: 1027-1047.

Rafiei Renani, H., Martin, C.D. and Hudson, R. 2016. Back Analysis of Rock Mass Displacements Around a Deep Shaft Using Two- and Three-Dimensional Continuum Modeling. *Rock Mechanics and Rock Engineering*, 49: 1313–1327.

Singh, M. and Singh, B. 1992. Correlation between Observed Support Pressure and Rock Mass Quality. *Tunnelling & Underground Space Technology*, 7(1): 59-74.

Vlachopoulos, N. and Diederichs, M.S. 2014. Appropriate Uses and Practical Limitations of 2D Numerical Analysis of Tunnels and Tunnel Support Response. Geotechnical and Geological Engineering, 32: 469-488.

Yu, Z., Kulatilake, P. H. S. W. and Jiang, F. 2012. Effect of Tunnel Shape and Support System on Stability of a Tunnel in a Deep Coal Mine in China. *Geotechnical and Geological Engineering*, 30(2): 383-394

Zou, D.H. 2004. Rock Bolt Loading Mechanism, SINOROCK 2002 - International Symposium on Rock Mechanics. Shanxi, China, (3A 08) on CD-ROM.

Zou, D.H. 2020. *Applied Rock Mechanics and Ground Stability*, 2nd ed., Canamaple Academia Services, Halifax, NS, Canada.